RSC Advances

PAPER

View Article Online
View Journal | View Issue

Cite this: *RSC Adv.*, 2024, **14**, 37797

Can selenenyl sulfides be a substrate of glutathione reductase enzyme? A theoretical insight†

Vishnu Rama Chari [ab] and Raghu Nath Behera [*a]

Received 18th September 2024
Accepted 6th November 2024

DOI: 10.1039/d4ra06738j

rsc.li/rsc-advances

Glutathione reductase (GR) catalyzes the reduction of glutathione disulfide (GSSG) to glutathione. As selenium is a congener of sulfur, the possibility of reducing selenenyl sulfide (RSeSG) at the catalytic site of GR has been investigated using density functional theory. Calculations on the redox potential and the Se–S bond strength of some studied RSeSG compounds with a phenyl selenide backbone suggested that the unsubstituted and amine-based selenenyl sulfide intermediates could have a promising tendency to be reduced at the catalytic site of GR.

1 Introduction

Glutathione peroxidase (GPx) plays an important role in regulating cellular oxidative stress. The enzymes in this family contain selenium in their active sites. In the catalytic cycle of GPx (Fig. 1), selenol (RSeH) is oxidized by reactive oxygen species (ROS), such as hydrogen peroxide or organic peroxides, to form selenenic acid (RSeOH). The elimination of ROS is followed by the regeneration of the catalyst in two essential events: regeneration of RSeH from RSeOH and regeneration of glutathione (GSH). The regeneration of RSeH proceeds through reduction of RSeOH to an important intermediate, selenenyl sulfide (RSeSG). This RSeSG is further reduced to selenol by another GSH molecule, forming glutathione disulfide (GSSG). GSH serves as the reagent necessary for regenerating the selenol in its reduced form (RSeH). In the cellular environment, GSSG is reduced back to GSH by glutathione reductase (GR) in the presence of NADPH[1–4] as depicted in eqn (1a). During this redox process, cysteines in the GR are oxidized to disulfides (eqn (1b)), and consequently, GSSG is reduced to two molecules of GSH (eqn (1c)).

$$\mathrm{GSSG} + \mathrm{GR}^{\mathrm{SH}}_{\mathrm{SH}} \rightleftharpoons 2\mathrm{GSH} + \mathrm{GR}^{\mathrm{S}}_{\mathrm{S}}] \quad (1a)$$

$$\text{Half reaction 1}: \mathrm{GR}^{\mathrm{SH}}_{\mathrm{SH}} \rightleftharpoons \mathrm{GR}^{\mathrm{S}}_{\mathrm{S}}] + 2\mathrm{H}^+ + 2\mathrm{e}^- \quad (1b)$$

$$\text{Half reaction 2}: \mathrm{GSSG} + 2\mathrm{H}^+ + 2\mathrm{e}^- \rightleftharpoons 2\mathrm{GSH} \quad (1c)$$

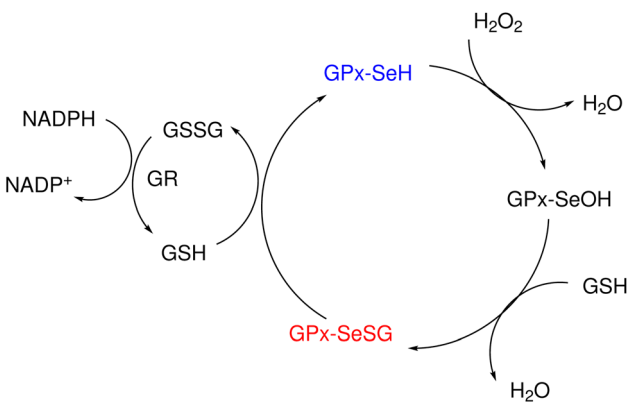

Fig. 1 Experimentally suggested mechanism for the catalytic cycle of GPx.

The Se–S bond appears naturally during the catalytic cycle of GPx when selenocysteine interacts with GSH in the active site of GPx. Besides GPx, the Se–S bond in selenenyl sulfides (RSe–SR′) is crucial in several other biological antioxidant regeneration enzymes such as thioredoxins.[5,6] However, in many cases, this bond is inherently unstable under standard atmospheric pressures and temperatures, posing significant challenges in studying its properties.[2] Previous studies[7,8] have demonstrated that compounds containing Se–S bonds exhibit antioxidant capabilities in animal studies. Moreover, selenenyl sulfides have emerged as promising agrochemical candidates[9] and have shown potential to act as antiviral inhibitors.[10]

After the successful discovery of ebselen as an antioxidant and anti-inflammatory drug, many small organoselenium compounds have been studied which mimic the antioxidant activity of GPx enzymes,[11,12] and many of them show a catalytic cycle similar to the (GPx) enzymes.[13–15] Their GPx-like activity has been evaluated using chemical, biochemical or electrochemical assays. The chemical assay is based on the rate of oxidation of an organic thiol (*e.g.* thiophenol (PhSH)) which

[a]*Department of Chemistry, Birla Institute of Technology and Science, Pilani, K. K. Birla Goa Campus, Zuarinagar, Goa 403726, India. E-mail: rbehera@goa.bits-pilani.ac.in*
[b]*School of Chemical Sciences, Goa University, Taleigao Plateau 403206, Goa, India*

† Electronic supplementary information (ESI) available. See DOI: https://doi.org/10.1039/d4ra06738j

forms the corresponding selenenyl sulfide RSeSPh, an important intermediate in the GPx-like catalytic cycle. This commonly used assay is prone to a thiol-exchange reaction when the Se atom in the selenenyl sulfide is more electrophilic than the S atom of the incoming thiol,[12,16] thus limiting its usefulness. The coupled reductase assay involves the reduction of GSSG by GR in the presence of GSH and NADPH.[4,17–20] This biochemical assay mimics the biological conditions in which the GPx enzymes function and is not limited by the thiol-exchange reaction. On the other hand, the electrochemical assay directly measures the rate of peroxide reduction employing a hydrogen peroxide selective electrode, which is capable of working in diverse thiol substrates and is free of any potential artefacts arising due to interaction of the organoselenium compound with any components of the assay.[21]

While comparing the activity of ebselen and diphenyldiselenide using an electrochemical assay and coupled reductase assay, Giles *et al.*[21] observed a two- to four-fold higher activity in the case of the coupled reductase assay. The observed increase in the activity for the coupled reductase assay compared to that of the electrochemical assay was proposed due to the interaction of the organoselenium compounds with GR. In a recent study,[22] it was observed that some of the derivatives of ebselen lacked thiophenol assay activity, while they showed similar or better activity in the coupled reductase assay. A similar observation was recorded by Yu *et al.*,[23] who suggested that the selenenyl sulfide intermediate could be responsible for showing the activity in the coupled reductase assay for the mimics, which lacked the activity in the thiophenol assay. Employing a molecular docking study, they showed that there is a possibility for a RSeSG-type intermediate to react at the catalytic site of GR, leading to the production of GSH and RSeH. This process is similar to the regeneration of two GSH molecules from GSSG at the active site of GR within the enzymatic cycle (eqn (1c)). These findings imply that RSeSG could mimic the behaviour of GSSG at the catalytic site of GR.

Based on these observations, we hypothesise that selenenyl sulfide can act as a substrate to GR. Accordingly, we consider the plausible redox reactions given in eqn (2a)–(2c) to model the conversion of RSeSG to RSeH (hereafter eqn (2c) will be denoted as RSeSG|(RSeH + GSH)). We have chosen RSeSG-type intermediates belonging to diphenyl diselenide **1a**, amine-based diselenides **2a** to **5a**, and ebselene-based **6a** to **8a** (amides) mimics for the investigation. The studied RSeSG intermediates, along with the parent GPx mimics, are given in Fig. 2. Factors influencing the catalyst regeneration include the redox potential of RSeSG|(RSeH + GSH) and the ease with which the Se–S bond breaks, *etc.*, have been investigated.

$$\mathrm{RSeSG} + \mathrm{GR}_{\mathrm{SH}}^{\mathrm{SH}} \rightleftharpoons \mathrm{RSeH} + \mathrm{GSH} + \mathrm{GR}_{\mathrm{S}}^{\mathrm{S}}] \quad (2a)$$

$$\text{Half reaction 1}: \mathrm{GR}_{\mathrm{SH}}^{\mathrm{SH}} \rightleftharpoons \mathrm{GR}_{\mathrm{S}}^{\mathrm{S}}] + 2\mathrm{H}^{+} + 2\mathrm{e}^{-} \quad (2b)$$

$$\text{Half reaction 2}: \mathrm{RSeSG} + 2\mathrm{H}^{+} + 2\mathrm{e}^{-} \rightleftharpoons \mathrm{RSeH} + \mathrm{GSH} \quad (2c)$$

2 Computational methodology

Geometry optimization of all the studied compounds was carried out using Gaussian 16.[24] Unless specified, all the calculations were performed at the M06-2X/6-311++g(2df,2pd) level of theory. Frequency calculations were conducted to verify that the optimized geometry has no imaginary frequency and, thus, is a minimum on the potential-energy surface. The solvent effect was modeled using the self-consistent reaction field (SCRF) approach utilizing the polarizable continuum model (PCM) with water as the solvent. The free energy of species in the solvent was calculated from the corresponding gas-phase geometries using a single-point calculation.[25] The non-covalent interactions in the intermediates were studied using NBO analysis as implemented in Gaussian 16.

The standard reduction potential (E°_{abs}) of the half-reaction

$$\mathrm{A(s)} + n_{\mathrm{e}}e_{\mathrm{g}}^{-} \rightleftharpoons \mathrm{B(s)} \quad (3)$$

can be calculated from its standard state free energy (SFE) from the relation

$$\Delta_{\mathrm{r}}G^{\circ}(\mathrm{A|B}) = -n_{\mathrm{e}}FE^{\circ}_{\mathrm{abs}}(\mathrm{A|B}), \quad (4)$$

where the oxidized species A gets reduced to B in the reaction by exchanging n_{e} number of electrons. "s" and "g" in the subscript or parentheses represents the species in solution and the gas phase, respectively. F is the Faraday constant.

The SFE of a reaction in solution ($\Delta_{\mathrm{r}}G^{\circ}_{\mathrm{s}}$) can be calculated from its corresponding gas-phase SFE ($\Delta_{\mathrm{r}}G^{\circ}_{\mathrm{g}}$) using the thermodynamic (Born–Haber) cycle (Fig. 3) as follows:[26–28]

$$\Delta_{\mathrm{r}}G^{\circ}_{\mathrm{s}}(\mathrm{A|B}) = \Delta_{\mathrm{r}}G^{\circ}_{\mathrm{g}}(\mathrm{A|B}) + \sum_{i}\Delta G^{\circ}_{\mathrm{s}}(B_i) - \sum_{i}\Delta G^{\circ}_{\mathrm{s}}(A_i), \quad (5)$$

where the 2nd and 3rd terms on the RHS represent the SFE of solvation for the products and the reactants, respectively. The index i goes over all the reactants or products.

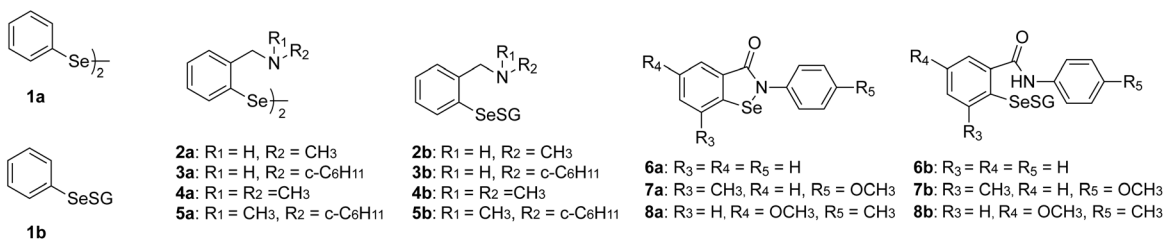

Fig. 2 Nomenclature of the parent GPx mimics (**1a–8a**) and the corresponding selenenyl sulfide intermediates (**1b–8b**) that were investigated.

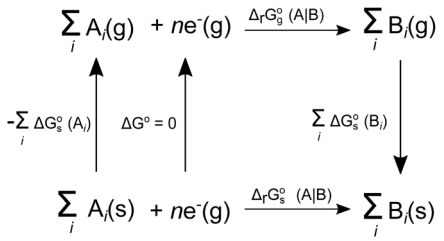

Fig. 3 Thermodynamic cycle designed to calculate $\Delta_r G_s^\circ$(A|B). Here, $\sum_i A_i$ = GSSG + 2H$^+$ (or RSeSG + 2H$^+$) and $\sum_i B_i$ = 2GSH (or RSeH + GSH) for the half-reaction (1c) (or (2c)).

The difference in SFE between the gas-phase reference state (1 atm, 24.46 L at 298.15 K) and that of the PCM solvation calculation (1 M) is calculated as per eqn (6):[27]

$$\Delta_r G_g^\circ(\mathrm{A|B})(1\ \mathrm{M}) = \Delta_r G_g^\circ(\mathrm{A|B})(1\ \mathrm{atm}) + \Delta nRT\ \ln(24.46), \quad (6)$$

where Δn is the net change of moles in Fig. 3, R is the gas constant and T is absolute temperature. The standard redox potential relative to the standard hydrogen electrode (SHE) for (A|B) can be expressed according to eqn (7).

$$\begin{aligned} E_{\mathrm{rel,SHE}}^\circ(\mathrm{A|B}) &= E_{\mathrm{abs}}^\circ(\mathrm{A|B}) - E_{\mathrm{abs}}^\circ(\mathrm{SHE}) \\ &= -\frac{\Delta_r G_s^\circ(\mathrm{A|B})(1\ \mathrm{M})}{n_e F} - E_{\mathrm{abs}}^\circ(\mathrm{SHE}) \end{aligned} \quad (7)$$

We have used $\Delta G_s^\circ(\mathrm{H^+}) = -1091.0$ kJ mol^{-1},[26,29] $\Delta G_g^\circ(\mathrm{H^+}) = -26.3$ kJ mol^{-1} [27,30] and $E_{\mathrm{abs}}^\circ(\mathrm{SHE}) = 4.42$ V [26] at $T = 298.15$ K in this work.

The homolytic bond-dissociation energy (BDE) of the X–Y bond is calculated using the following equation:

$$\mathrm{BDE} = \Delta_f H(\mathrm{R_1X}) + \Delta_f H(\mathrm{R_2Y}) - \Delta_f H(\mathrm{R_1X\text{–}YR_2}), \quad (8)$$

in which $\mathrm{R_1X–YR_2}$ is the neutral molecule, and $\mathrm{R_1X}$ and $\mathrm{R_2Y}$ are the corresponding radicals. The geometries of the radicals were optimized at the unrestricted M06-2X/6-311++g(2df,2pd) level of theory.

3 Results and discussion

3.1 Redox potential and feasibility of the reaction of RSeSG at GR

The method for calculating the redox potential of RSeSG (shown in Fig. 2) follows a similar approach to that used for the GSSG, as outlined in the ESI† (Justification of functionals). Similar to the GSSG|2GSH couple, the redox potentials of RSeSG|(RSeH + GSH) couple (eqn (2c)) were calculated from $\Delta_r G_s^\circ$(A|B), where $\sum_i A_i$ = RSeSG + 2H$^+$ and $\sum_i B_i$ = RSeH + GSH, using the thermodynamic cycle shown in Fig. 3 and are given in Table 1. The calculated redox potentials for amine-based selenenyl sulfides **2b** to **5b** are about 10–40 mV more positive than that for GSSG, whereas the ebselen-based selenenyl sulfide intermediates exhibit redox potential values that are about 110–150 mV more negative than that for GSSG. The reported values of the redox potentials of selenenyl sulfides depend on various conditions, and range from −0.381 to −0.215 V at pH = 7.[31–33]

More positive redox potentials (Table 1) of the amine-based intermediates (**2b** to **5b**) than those of GSSG or the ebselen-based selenenyl sulfide intermediates (**6b** to **8b**) indicate that the amine-based intermediates have a higher tendency to be reduced to form selenol – the active catalyst in the GPx-like catalytic cycle. For the amine-based intermediates **2b** to **5b**, the $r_{\mathrm{Se\cdots N}}$ distances are found to be smaller than the sum of their van der Waals radii[34] (r_{vdW}(Se) + r_{vdW}(N)), and also the N⋯Se–S angles are almost linear (173–175°) (see Table 1, and Fig. S1 and S2 in the ESI†) indicating the presence of non-covalent Se⋯N interactions. The strength of the (Se⋯N) interactions (which involve $n_{\mathrm{N}} \rightarrow \sigma^*_{\mathrm{Se-S}}$ orbitals)[35,36] obtained by the NBO second-order perturbation energy (E_2) are also given in Table 1. The Se⋯N interaction is relatively weaker in intermediates with secondary amino groups (**2b** and **3b**), compared to intermediates with tertiary amino groups (**4b** and **5b**). Thus, E_2 for these intermediates increases as the calculated redox potential decreases, indicating that a stronger Se⋯N interaction results in a weaker reducing ability of the selenenyl sulfide intermediates. Specifically, intermediates with a methyl group as the only substituent on the amino nitrogen, **2b** (8.11 kcal mol^{-1}, −0.252 V) and **4b** (9.74 kcal mol^{-1}, −0.264 V) exhibit a relatively weaker Se⋯N interaction and, consequently, more positive redox potentials compared to their counterparts with cyclohexyl substitution **3b** (9.20 kcal mol^{-1}, −0.257 V) and **5b** (10.56 kcal mol^{-1}, −0.280 V). This observation suggests that the presence of a cyclohexyl ring on the amino nitrogen enhances the Se⋯N interaction. The absence of Se⋯N non-covalent interactions in ebselen-based intermediates (**6b–8b**) could be a reason for showing relatively more negative redox potentials than glutathione.

To further understand the tendency of RSeSG reduction at the catalytic site of GR, we define a relative equilibrium constant K_{rel} as follows. The thiol–disulfide equilibrium represents a dynamic state where the rates of the forward and reverse reactions are balanced to sustain constant concentrations of reactants and products during the reduction of GSSG at GR as depicted in eqn (1a). The equilibrium constant K_{eq} is related to the standard free-energy change ΔG° and standard electrode potential through eqn (9):

$$K_{\mathrm{eq1}} = e^{-\frac{\Delta G^\circ}{RT}} = e^{\frac{n_e F E_1^\circ}{RT}}, \quad (9)$$

where $E_1^\circ = E_{\mathrm{GSSG|2GSH}}^\circ - E_{\mathrm{GR_S^S||GR_{SH}^{SH}}}^\circ$. Similarly, the equilibrium constant for the RSeSG reduction (eqn (2a)) can be written as

$$K_{\mathrm{eq2}} = e^{\frac{n_e F E_2^\circ}{RT}}, \quad (10)$$

where $E_2^\circ = E_{\mathrm{RSeSG|(GSH+RSeH)}}^\circ - E_{\mathrm{GR_S^S||GR_{SH}^{SH}}}^\circ$. Assuming that the RSeSG and GSSG interact similarly with the enzyme, the $E_{\mathrm{GR_S^S||GR_{SH}^{SH}}}^\circ$ terms may cancel out, and an equilibrium constant for RSeSG conversion relative to that of GSSG conversion may be defined as

$$K_{\mathrm{rel}} = \frac{K_{\mathrm{eq2}}}{K_{\mathrm{eq1}}} = e^{\frac{n_e F}{RT}\left(E_2^\circ - E_1^\circ\right)}. \quad (11)$$

Table 1 Important thermodynamic and structural parameters[a] of the studied compounds using the M06-2X/6-311++g(2df,2pd) level of theory

Compd	$E^{\circ}_{rel,SHE}(A\|B)$[b]	K_{rel}[c]	$r_{S-Se/S}$[d]	$r_{N\cdots Se}$[d]	$\angle_{N\cdots Se-S}$[d]	BDE[e]	E_2[f]
1b	−0.251	1.95×10^{1}	2.178	—	—	56.8	—
2b	−0.252	1.88×10^{1}	2.204	2.833	173.6	53.6	8.11
3b	−0.257	1.24×10^{1}	2.207	2.792	173.9	53.9	9.20
4b	−0.264	6.96	2.209	2.770	174.5	53.2	9.74
5b	−0.280	2.02	2.212	2.726	175.4	53.5	10.56
GSSG	−0.289	1.00	2.055	—	—	65.3	—
6b	−0.396	2.50×10^{-4}	2.194	—	—	63.6	—
7b	−0.404	1.38×10^{-4}	2.198	—	—	62.1	—
8b	−0.443	6.42×10^{-6}	2.196	—	—	69.1	—
2′b	−0.231	9.78×10^{1}	2.204	2.925	159.0	52.9	4.85

[a] Illustrative figures (Fig. S1 and S2) showing the structural parameters are included in the ESI.† [b] Calculated redox potentials, $E^{\circ}_{rel,SHE}(A|B)$ at pH = 7 in volts; here A|B is either the RSeSG|(RSeH + GSH) or GSSG|2GSH couple. [c] K_{rel} represents the relative equilibrium constant with respect to that of the GSSG|2GSH pair. [d] S–Se/S, and N⋯Se, bond distance in Å, bond angle N⋯Se–S in degrees. [e] The gas-phase bond dissociation energy (BDE) for the S–Se/S bond in kcal mol^{-1}. [f] Second-order perturbation energy (E_2) from NBO for the Se⋯N non-covalent interactions in kcal mol^{-1}.

The relative equilibrium constant, K_{rel} depends on the redox potentials of RSeSG and GSSG and indicates the ability of RSeSG to be reduced at the active site of GR in comparison to GSSG. The calculated values of K_{rel} (Table 1) imply that the unsubstituted phenyl selenide intermediate **1b** would have a higher tendency to be reduced at the GR, then the secondary-amine-containing analogues **2b** and **3b**, followed by the tertiary amines **4b** and **5b**. Conversely, ebselen and its substituted compounds (**6b** to **8b**) show a much lower tendency (K_{rel}) to be reduced compared to GSSG. The compounds having a relatively positive redox potential tend to reach equilibrium rapidly.[33]

We have carried out a molecular docking study taking GSSG and RSeSG (as ligands) at the active site of GR. This study shows that many of the studied ligands can approach the active site of GR in a range of 5 Å, indicating that there is a possibility of interactions between some of the RSeSG and GR. The details are given in the ESI (Fig. S3, S4, and Table S3).†

3.2 Bond dissociation energy

To facilitate the easy reduction of selenenyl sulfides (RSeSG) to selenol (RSeH) and thiol (GSH) at the catalytic site of GR, the RSeSG intermediates should not only possess a more positive redox potential, but also have a weaker Se–S bond. The calculated value of BDE for the disulfide bond in GSSG is found to be 65.3 kcal mol^{-1}, which is comparable to the experimental value of a typical disulfide bond (*e.g.* 66.2 kcal mol^{-1} for dialkyl disulfide[37]). The calculated Se–S BDE data and bond distances are presented in Table 1. The Se–S BDEs of all the RSeSG compounds (except **8b**) are lower than the S–S BDE of GSSG. Notably, all our studied intermediates contain a phenyl selenide backbone. Compared to the parent phenyl selenenyl sulfide **1b**, the amine-substituted selenenyl sulfides (**2b** to **5b**) exhibit Se–S BDEs that are about 3 kcal mol^{-1} lower (ranging from 53.2 to 53.9 kcal mol^{-1}), while those amide-substituted (ebselen-based) selenenyl sulfides (**6b** to **8b**) showed BDEs that are higher by amounts ranging from approximately 5 to 12 kcal mol^{-1} (with values ranging from 62.1 to 69.1 kcal mol^{-1}).

Among the amide-substituted (ebselen-based) compounds, **6b** shows a relatively more positive redox potential (than **7b** or **8b**), while **7b** has the lowest BDE (compared to **6b** and **8b**). Using a coupled reductase assay it was reported recently that **7a** (the parent compound of **7b**) showed better activity than those of **6a** and **8a** (about 1.6 times better than that of **6a**, while **6a** showed an activity about 1.2 times higher than **8a**).[22] Since RSeSG is formed during the coupled reductase assay, a lower activity of **8a** could be ascribed to its relatively higher Se–S BDE. However, the relatively better activity of **7a** compared to **6a** indicated that the interplay of redox potential and Se–S BDE would play a crucial role during the reduction of RSeSG at GR.

The amine-substituted compounds (**2b** to **5b**) showed the lowest Se–S BDEs, while the parent phenyl selenenyl sulfide (**1b**) showed the most positive redox potential. The lower BDEs of **2b** to **5b** may be attributed to the presence of Se⋯N non-covalent interactions, which is known to weaken the Se–S bond.[36,38] As the strength of these interactions (E_2) decreases, the BDEs change a little, while the redox potential shifts towards more positive values (reaching close to that of **1b**). This indicates that the strength of the Se⋯N interactions altered not only the Se–S BDE but also the redox potential of RSeSG. To test this hypothesis, we chose the parent compound **2′a**, which was found to give better catalytic activity in a thiophenol assay during previous testing of this family of amine-based GPx mimics.[39] The results on its selenenyl sulfide intermediate **2′b** are given in Table 1 and Fig. 4. As expected, **2′b** showed the weakest Se⋯N interaction ($E_2 = 4.85$ kcal mol^{-1}), the lowest Se–S BDE (52.9 kcal mol^{-1}), and the most positive redox potential (–0.231 V). Also, we find a very good correlation ($R^2 = 0.93$) between the strength of the Se⋯N interaction and the redox potential among the studied amine-substituted RSeSG compounds (Fig. 4). Although it is reported that ebselen-based compounds exhibit Se⋯O interactions,[40] NBO analysis of the ebselen-based compounds under study did not show any Se⋯O or Se⋯N interactions. The Se⋯O distances in the present case are in the range of 3.07 to 3.13 Å (Fig. S2†).

Thus, the presence of Se⋯N non-covalent interactions in RSeSG lowers the Se–S BDE, while a moderate (not too strong)

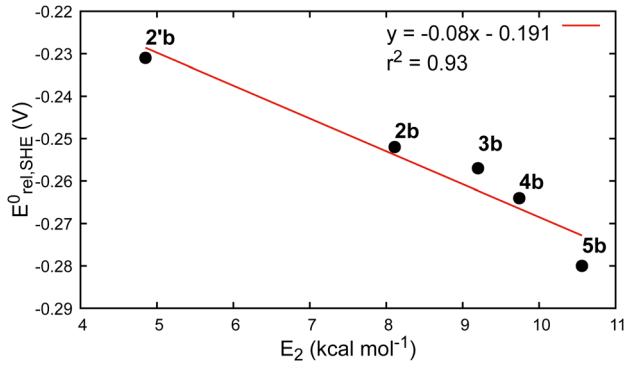

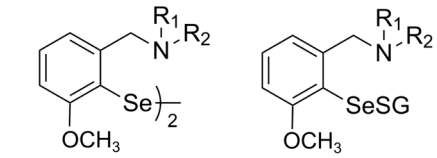

2'a: R_1 = H, R_2 = CH_3 **2'b**: R_1 = H, R_2 = CH_3

Fig. 4 Correlations between the strength of the Se···N non-covalent interaction (E_2) and the calculated redox potential for amine-based RSeSGs (top). Structure of **2′a** and **2′b** (bottom).

value of such interactions results in a higher positive redox potential and may modulate its peroxidase activity. This prediction is consistent with the literature results that some of the most successful GPx mimics contain a selenium–nitrogen interaction (Se–N bond or a close Se···N interaction).[38] Mimics with weaker Se···N interactions (E_2 < ~7 kcal mol^{-1}) showed relatively higher activities, while those with strong Se···N interactions (E_2 > ~11 kcal mol^{-1}) showed relatively lower activities.[41] The presence of strong Se···N interactions in the selenenyl sulfide intermediates has shown a preference for the thiol-exchange reactions over the regeneration of active selenol (RSeH), thereby reducing the GPx activity significantly.[12,16]

4 Conclusions

In summary, we have explored the possibility of reduction of potential selenenyl sulfide intermediates (RSeSG) at the catalytic site of GR. The diphenyl diselenide-based selenenyl sulfides (**1b** to **5b**, and **2′b**) showed more positive redox potentials and lower Se–S BDEs than GSSG. The molecular docking study indicated a closer approach of some of these RSeSG compounds in proximity to the active site of GR (~5 Å), suggesting that these species can potentially be reduced at the catalytic site of GR. The presence of Se···N non-covalent interactions alters both the Se–S BDEs as well as the redox potentials of RSeSG. Thus, fine-tuning the strength of these non-covalent interactions could be a way to modulate the GPx activity and identify more potent antioxidants.

Data availability

The data supporting this article have been included as part of the ESI.†

Author contributions

Vishnu Rama Chari: conceptualization, investigation, writing – original draft, visualization. Raghu Nath Behera: conceptualization, investigation, writing – review & editing, funding acquisition, supervision.

Conflicts of interest

The authors declare that they have no known competing financial interests or personal relationships that could have appeared to influence the work reported in this paper.

Acknowledgements

This work was supported by the Science and Engineering Research Board (Project No. EMR/2016/003210). We acknowledge the DST-FIST supported computational facility to the Department of Chemistry, and the HPC facility of Birla Institute of Technology and Science Pilani, K. K. Birla Goa Campus for this work. VRC is thankful to UGC-SAP and DST-FIST funding to School of Chemical Sciences, Goa University. We thank the anonymous reviewers for their helpful comments and suggestions.

Notes and references

1 L. Flohé, Glutathione Peroxidase, in, *Ciba Foundation Symposium 65 - Oxygen Free Radicals and Tissue Damage*, ed. D. W. Fitzsimons, 1979, pp. 95–122.
2 A. Hamsath and M. Xian, *Antioxid. Redox Signaling*, 2020, **33**, 1143–1157.
3 E. Lubos, J. Loscalzo and D. E. Handy, *Antioxid. Redox Signaling*, 2011, **15**, 1957–1997.
4 M. D. Tiezza, G. Ribaudo and L. Orian, *Curr. Org. Chem.*, 2019, **23**, 1381–1402.
5 B. K. Sarma and G. Mugesh, *Org. Biomol. Chem.*, 2008, **6**, 965–974.
6 C. Gallo-Rodriguez and J. B. Rodriguez, *ChemMedChem*, 2024, **19**, e202400063.
7 C. V. Rao, C. Wang, B. Simi, J. G. Rodriguez, I. Cooma, K. El-Bayoumy and B. S. Reddy, *Cancer Res.*, 2001, **61**, 3647–3652.
8 M. Prigol, E. A. Wilhelm, C. C. Schneider and C. W. Nogueira, *Chem.-Biol. Interact.*, 2008, **176**, 129–136.
9 M.-H. Shang, X.-W. Sun, H.-L. Wang, H.-R. Li, J.-S. Zhang, L.-Z. Wang, S.-J. Yu, X. Zhang, L.-X. Xiong, Y.-H. Li, *et al.*, *Pest Manage. Sci.*, 2023, **79**, 1885–1896.
10 J.-Y. Tang, S. Dai, X. Wang, M. Zhang, J.-R. Shi, Y.-X. Hong, Z.-J. Sun, H.-Q. Dai and J.-G. Wang, *Arabian J. Chem.*, 2024, **17**, 105713.
11 N. V. Barbosa, C. W. Nogueira, P. A. Nogara, A. F. de Bem, M. Aschner and J. B. Rocha, *Metallomics*, 2017, **9**, 1703–1734.
12 K. P. Bhabak and G. Mugesh, *Acc. Chem. Res.*, 2010, **43**, 1408–1419.
13 M. Iwaoka and S. Tomoda, *J. Am. Chem. Soc.*, 1994, **116**, 2557–2561.

14 G. S. Heverly-Coulson and R. J. Boyd, *J. Phys. Chem. A*, 2010, **114**, 1996–2000.
15 J. K. Pearson and R. J. Boyd, *J. Phys. Chem. A*, 2007, **111**, 3152–3160.
16 B. K. Sarma and G. Mugesh, *J. Am. Chem. Soc.*, 2005, **127**, 11477–11485.
17 V. P. Singh, J.-f. Poon, R. J. Butcher, X. Lu, G. Mestres, M. K. Ott and L. Engman, *J. Org. Chem.*, 2015, **80**, 7385–7395.
18 M. Kumar and V. P. Singh, *New J. Chem.*, 2022, **46**, 12010–12022.
19 G. Mugesh and H. B. Singh, *Chem. Soc. Rev.*, 2000, **29**, 347–357.
20 E. F. Pai and G. E. Schulz, *J. Biol. Chem.*, 1983, **258**, 1752–1757.
21 N. M. Giles, S. Kumari, R. A. Stamm, S. Patel and G. I. Giles, *Anal. Biochem.*, 2012, **429**, 103–107.
22 M. Kumar, B. Chhillar, D. Verma, S. Nain and V. P. Singh, *J. Org. Chem.*, 2023, **88**, 4273–4285.
23 S.-C. Yu, I.-C. Kim, K.-J. Ri, J. Ri and H. Kuehn, *J. Inorg. Biochem.*, 2021, **215**, 111276.
24 M. J. Frisch, G. W. Trucks, H. B. Schlegel, G. E. Scuseria, M. A. Robb, J. R. Cheeseman, G. Scalmani, V. Barone, G. A. Petersson, H. Nakatsuji, X. Li, M. Caricato, A. V. Marenich, J. Bloino, B. G. Janesko, R. Gomperts, B. Mennucci, H. P. Hratchian, J. V. Ortiz, A. F. Izmaylov, J. L. Sonnenberg, D. Williams-Young, F. Ding, F. Lipparini, F. Egidi, J. Goings, B. Peng, A. Petrone, T. Henderson, D. Ranasinghe, V. G. Zakrzewski, J. Gao, N. Rega, G. Zheng, W. Liang, M. Hada, M. Ehara, K. Toyota, R. Fukuda, J. Hasegawa, M. Ishida, T. Nakajima, Y. Honda, O. Kitao, H. Nakai, T. Vreven, K. Throssell, J. A. Montgomery Jr, J. E. Peralta, F. Ogliaro, M. J. Bearpark, J. J. Heyd, E. N. Brothers, K. N. Kudin, V. N. Staroverov, T. A. Keith, R. Kobayashi, J. Normand, K. Raghavachari, A. P. Rendell, J. C. Burant, S. S. Iyengar, J. Tomasi, M. Cossi, J. M. Millam, M. Klene, C. Adamo, R. Cammi, J. W. Ochterski, R. L. Martin, K. Morokuma, O. Farkas, J. B. Foresman and D. J. Fox, *Gaussian-16 Revision C.01*, Gaussian Inc., Wallingford CT, 2016.
25 M.-H. Baik and R. A. Friesner, *J. Phys. Chem. A*, 2002, **106**, 7407–7412.
26 A. V. Marenich, J. Ho, M. L. Coote, C. J. Cramer and D. G. Truhlar, *Phys. Chem. Chem. Phys.*, 2014, **16**, 15068–15106.
27 H. Mohammad-Shiri, M. Ghaemi, S. Riahi and A. Akbari-Sehat, *Int. J. Electrochem. Sci.*, 2011, **6**, 317–336.
28 O. Hammerich and B. Speiser, *Organic Electrochemistry: Revised and Expanded*, CRC Press, 2015.
29 M. D. Liptak, K. C. Gross, P. G. Seybold, S. Feldgus and G. C. Shields, *J. Am. Chem. Soc.*, 2002, **124**, 6421–6427.
30 J. J. Fifen, Z. Dhaouadi and M. Nsangou, *J. Phys. Chem. A*, 2014, **118**, 11090–11097.
31 D. Besse, F. Siedler, T. Diercks, H. Kessler and L. Moroder, *Angew. Chem., Int. Ed. Engl.*, 1997, **36**, 883–885.
32 F. Li, P. B. Lutz, Y. Pepelyayeva, E. S. Arnér, C. A. Bayse and S. Rozovsky, *Proc. Natl. Acad. Sci. U. S. A.*, 2014, **111**, 6976–6981.
33 K. Arai, T. Matsunaga, H. Ueno, N. Akahoshi, Y. Sato, G. Chakrabarty, G. Mugesh and M. Iwaoka, *Chem.–Eur. J.*, 2019, **25**, 12751–12760.
34 A. v. Bondi, *J. Phys. Chem.*, 1964, **68**, 441–451.
35 A. Panda and R. N. Behera, *J. Hazard. Mater.*, 2014, **269**, 2–8.
36 R. N. Behera and A. Panda, *RSC Adv.*, 2012, **2**, 6948–6956.
37 Y.-R. Luo, *Comprehensive Handbook of Chemical Bond Energies*, CRC Press, 2007.
38 A. J. Mukherjee, S. S. Zade, H. B. Singh and R. B. Sunoj, *Chem. Rev.*, 2010, **110**, 4357–4416.
39 K. P. Bhabak and G. Mugesh, *Chem.–Eur. J.*, 2009, **15**, 9846–9854.
40 S. Antony and C. A. Bayse, *Inorg. Chem.*, 2011, **50**, 12075–12084.
41 K. P. Bhabak and G. Mugesh, *Chem.–Eur. J.*, 2008, **14**, 8640–8651.